Title: The Small GTPase OsRac1 forms two distinct immune receptor complexes containing the PRR OsCERK1 and the NLR Pit

Running head: OsRac1 forms two immune receptor complexes

Akira Akamatsu [1, 2, $], Masayuki Fujiwara [2, 3, $], Satoshi Hamada [2, $], Megumi Wakabayashi [2, 4], Ai Yao [2], Qiong Wang [5], Ken-ichi Kosami [6, 7], Thu Thi Dang [2, 6, 8], Takako Kaneko-Kawano [9], Ko Shimamoto [2], and Yoji Kawano [2, 6, 10, 11]

[1] Department of Bioscience, Kwansei Gakuin University, 2-1 Gakuen, Hyogo 669-1337, Japan

[2] Graduate School of Biological Sciences, Nara Institute of Science and Technology, Nara 630-0192, Japan

[3] Yanmar Holdings Co., Ltd., Osaka 530-8311, Japan

[4] Field Solutions North East Asia, Agronomic Operations Japan, Agronomic Technology Station East Japan, Bayer CropScience K.K., Yuki, Ibaraki 307-0001, Japan

[5] Department of Horticulture and Plant Protection, Yangzhou University, Yangzhou 225009, China

[6] CAS Center for Excellence in Molecular Plant Sciences, Shanghai Center for Plant Stress Biology, Chinese Academy of Sciences, Shanghai 201602, China

[7] Fruit Tree Research Center, Ehime Research Institute of Agriculture, Forestry and Fisheries, Matsuyama, Ehime 791-0112, Japan

[8] IRHS-UMR1345, Université d'Angers, INRAE, Institut Agro, SFR 4207 QuaSaV, 49071, Beaucouzé, France

[9] College of Pharmaceutical Sciences, Ritsumeikan University, Kusatsu, Shiga 525-8577, Japan

[10] Kihara Institute for Biological Research, Yokohama City University, Kanagawa 244-0813, Japan

[11] Institute of Plant Science and Resources, Okayama University, Okayama 710-0046, Japan

[$] These authors contributed equally to this work. Their names are in alphabetical order.

Correspondence should be addressed to: Yoji Kawano
Institute of Plant Science and Resources
Okayama University
2-20-1, Chuo, Kurashiki, Okayama 710-0046 Japan
Tel: +81-86-434-1242
E-mail: yoji.kawano@okayama-u.ac.jp

Abstract:

Plants employ two different types of immune receptors, cell surface pattern recognition receptors (PRRs) and intracellular nucleotide-binding and Leucine-rich repeat-containing proteins (NLRs), to cope with pathogen invasion. Both immune receptors often share similar downstream components and responses but it remains unknown whether a PRR and an NLR assemble into the same protein complex or two distinct receptor complexes. We have previously found that the small GTPase OsRac1 plays key roles in the signaling of OsCERK1, a PRR for fungal chitin, and of Pit, an NLR for rice blast fungus, and associates directly and indirectly with both of these immune receptors. In this study, using biochemical and bioimaging approaches, we reveal that OsRac1 formed two distinct receptor complexes with OsCERK1 and with Pit. Supporting this result, OsCERK1 and Pit utilized different transport systems for anchorage to the plasma membrane. Activation of OsCERK1 and Pit led to OsRac1 activation and, concomitantly, OsRac1 shifted from a small to a large protein complex fraction. We also found that the chaperone Hsp90 contributed to the proper transport of Pit to the plasma membrane and the immune induction of Pit. These findings illuminate how the PRR OsCERK1 and the NLR Pit orchestrate rice immunity through the small GTPase OsRac1.

Keywords: immunity, NLR, OsRac1, PRR, rice

Introduction

Plants utilize two layers of immune response to cope with pathogen infection. The first layer is known as pathogen-/microbe-associated molecular pattern (PAMP/MAMP)-triggered immunity (PTI/MTI), while the second layer is called effector-triggered immunity (ETI) (Dangl et al. 2013; Dodds and Rathjen 2010). PTI is triggered by transmembrane pattern recognition receptors (PRRs) and induces early responses (Couto and Zipfel 2016). Most PRRs are categorized into two protein families consisting of receptor-like kinases (RLKs) and receptor-like proteins (RLPs) (Monaghan and Zipfel 2012). RLKs perceive signals through their extracellular domains, transmit these signals to kinase domains, and phosphorylate their downstream intracellular signaling molecules. ETI is initiated by either direct or indirect recognition of pathogen effectors by the nucleotide-binding domain and leucine-rich repeats (NLR) family proteins (Cui et al. 2015).

In at least some cases, PTI and ETI employ similar signaling machinery such as Ca^{2+} signaling, reactive oxygen species (ROS) generation, transcriptional reprogramming, and MAP kinase (MAPK) cascade activation (Peng et al. 2018; Tsuda et al. 2013). Transcriptome analysis has revealed that the sets of genes induced by PTI and ETI overlap. However, the immune responses induced by ETI are generally more rapid, prolonged, and robust than those induced by PTI (Dodds and Rathjen 2010; Tao et al. 2003; Thomma et al. 2011; Tsuda and Katagiri 2010). Moreover, PRRs and NLRs require each other to effect robust disease resistance (N'gou et al. 2020; Yuan et al. 2020). These results suggest that PTI and ETI share the same or similar signaling machinery, while their dynamics and strength are different. Qi et al. previously demonstrated that an *Arabidopsis* PRR, FLAGELLIN-SENSING 2 (FLS2), is physically associated with three plasma membrane (PM)-localized NLR proteins, RPS2, RPM1, and RPS5 (Qi et al.

2011). However, it is currently unclear whether physical interaction between PRRs and NLRs is a general feature and how two different types of immune receptors, PRRs and NLRs, induce similar responses.

Heat shock proteins (Hsps) are abundant and highly conserved proteins that accumulate in response to various stresses and serve as molecular chaperones for diverse client proteins. Hsp90 associates with many co-chaperones and cofactors to promote proper folding and maturation of client proteins (Pearl and Prodromou 2006). Previous studies have shown that Hsp90 plays critical roles in NLR functions. Indeed, suppression of HSP90 function leads to increased susceptibility to pathogens (Hubert et al. 2003; Lu et al. 2003). Hsp90 forms a complex(es) with co-chaperones such as Suppressor of G2 allele of skp1 (SGT1) and required for Mla12 resistance1 (RAR1) (Shirasu et al. 1999; Takahashi et al. 2003), and contributes to the stabilization of NLR proteins (Kadota and Shirasu 2012). Hsp90.7, an ER-localized Hsp, is required for the correct folding and/or complex formation of the two RLKs CLAVATA 1 and 2 to control shoot and floral meristem development (Ishiguro et al. 2002).

Members of the small GTPase Rac/Rop family act as molecular switches and play crucial roles in a variety of plant physiological processes (Berken 2006; Nibau et al. 2006). The small GTPase OsRac1 functions as a key regulator in both PTI and ETI in rice (Kawano et al. 2010b; Kawano et al. 2014b; Kawano and Shimamoto 2013). OsRac1 contributes to PTI triggered by two elicitors, chitin and sphingolipid, derived from fungal pathogens. We have also revealed that an OsCERK1–OsRacGEF1–OsRac1 module is involved in early signaling for chitin-induced immunity (Akamatsu et al. 2015; Akamatsu et al. 2013). After sensing chitin, the chitin receptor complex containing the RLP OsCEBiP and the RLK OsCERK1 phosphorylates OsRacGEF1, which is a PRONE

family activator protein of OsRac1. OsCERK1-dependent phosphorylation of OsRacGEF1 leads to OsRac1 activation, resulting in the induction of immune responses. Hsp90 and its co-chaperone Hop/Sti1 complex contribute to the maturation and intracellular transport of the OsCERK1 complex (Chen et al. 2010a). Moreover, OsRac1 also forms a complex(es) with various proteins including Hsp70, the scaffold protein OsRACK1, the lignin biosynthesis enzyme OsCCR1, and OsMPK6 (Kawasaki et al. 2006; Kim et al. 2012; Lieberherr et al. 2005; Nakashima et al. 2008; Thao et al. 2007). In ETI, NLR proteins employ a different mechanism to elicit OsRac1 activation from PRRs (Kawano et al. 2010a; Wang et al. 2018). Two NLR proteins, Pit and Pia, for rice blast fungus directly bind to OsSPK1, which is a DOCK family activator protein for OsRac1, and induce OsRac1 activation through OsSPK1, leading to disease resistance to rice blast fungus (Kawano et al. 2014a; Ono et al. 2001; Wang et al. 2018). So far, many players get involved in the immune complex(es) with OsRac1, however which components form a distinct complex(es) in PTI and ETI as well as their functions remain to be explored.

In this study, we demonstrated that OsRac1 formed two distinct immune receptor complexes with the RLK OsCERK1 and the NLR Pit. Chitin perception or induction of an active form of Pit made OsRac1 into an active form, which led to the redistribution of OsRac1 from a low to a high molecular weight complex. Hsp90 appears to play a critical role in the proper localization of Pit. These results shed light on the underlying molecular mechanisms of how PRRs and NLRs orchestrate rice immunity through the small GTPase OsRac1.

Results

Two distinct immune receptor complexes: the PRR OsCERK1 and the NLR Pit

The small GTPase OsRac1 functions as a downstream molecular switch for two different types of immune receptors, the PRR OsCERK1 and the NLR Pit (Akamatsu et al. 2013; Kawano et al. 2010a; Wang et al. 2018), and we therefore wondered whether the three proteins form a ternary complex or two distinct complexes. We performed an immunoprecipitation assay using rice suspension cells expressing *Myc-OsRac1* with *OsCERK1-FLAG* and/or *Pit-HA*. When OsCERK1-FLAG or Pit-HA was immunoprecipitated, OsRac1 coprecipitated with each (Fig. 1A). However, we observed no interaction between OsCERK1 and Pit even when we reciprocally precipitated both receptors, implying that OsCERK1 and Pit form two distinct immune receptor complexes with OsRac1. To validate this result in living cells, we employed two bioimaging methods. First, we tested for an interaction between OsCERK1 and Pit *in vivo* using bimolecular fluorescence complementation (BiFC) assays. To quantify the interactions in BiFC assays, we measured the frequency of reconstituted Venus-positive protoplasts in each combination of constructs. When OsCERK1 tagged with the N-terminal domain (aa 1-154) of Venus (OsCERK1-Vn) and Pit tagged with the C-terminal domain (aa 155-238) of Venus (Pit-Vc) were co-expressed in rice protoplasts, Venus fluorescence was not detected under conditions in which the known interactions between OsRac1 and Pit as well as OsCERK1 and Hop/Sti1 were confirmed (Chen et al. 2010a; Kawano et al. 2010a) (Fig. 1B). Since we have previously shown that both Pit and OsRac1 are localized at the plasma membrane through palmitoylation, a lipid modification (Chen et al. 2010b; Kawano et al. 2014a; Ono et al. 2001), we further tested the distribution of OsCERK1 and Pit in living cells using variable angle epifluorescence microscopy, also called

variable incidence angle fluorescence microscopy (VIAFM) (Fujimoto et al. 2010; Konopka and Bednarek 2008). VIAFM is a derivative of total internal reflection fluorescence microscopy employing an evanescent wave that excites fluorescent proteins selectively in a region of the specimen beneath the glass-water interface, such as the plasma membrane and the cytoplasmic zone immediately beneath the plasma membrane of cells. We transfected rice protoplasts with *OsCERK1-mCherry* and *Pit-mGFP* vectors and observed the localization of the expressed proteins (Fig. 1C). OsCERK1-mCherry and Pit-mGFP showed small fluorescent particles, whereas there were no detectable particles in control mGFP-expressing cells (Supplemental Fig. 1D). The result of dual-fluorescence imaging using OsCERK1-mCherry and Pit-WT-mGFP clearly demonstrated that almost none of the OsCERK1-mCherry and Pit-mCherry particles overlapped with each other (Fig. 1C). On the other hand, OsCERK1-mCherry co-localized well with mEGFP-OsCEBiP, a co-chitin receptor (Supplemental Fig. 1E–G). Taken together, these results indicate that OsCERK1 and Pit form two different immune complexes with OsRac1.

Different signaling components and intracellular transport of OsCERK1 and Pit

Based on a number of protein–protein interactions and functional studies, we have previously demonstrated that OsCERK1 directly binds to chaperone Hsp90 and co-chaperone Hop/Sti1a (Chen et al. 2010a). Moreover, OsRac1 interacts either directly or indirectly with Hsp90, its co-chaperones Hop/Sti1a, SGT1, and RAR1, the scaffold protein RACK1A, and MAP kinase MPK6, and these components play important roles in both PTI and ETI (Akamatsu et al. 2013; Chen et al. 2010a; Kawano et al. 2010a; Lieberherr et al. 2005; Nakashima et al. 2008; Thao et al. 2007). To identify the

components of OsCERK1 and Pit complexes, we performed an immunoprecipitation assay using rice suspension cells. The two different immune receptor complexes contain shared components including Hsp90, Hop/Sti1, and OsRac1, but they do not include the OsRac1 interactors RACK1A, RAR1, or MPK6 (Fig. 2A and 2B). Interestingly, SGT1 is a specific component in the Pit complex (Fig. 2B).

Generally, small GTPase Rac/Rop family proteins are localized at the plasma membrane as a result of post-translational modification (Ono et al. 2001; Yalovsky et al. 2008). We have previously shown that OsRac1 localizes predominantly at the PM (Chen et al. 2010a), and that Hop/Sti1a and Hsp90 are present in the PM-rich fraction (Chen et al. 2010b). To more precisely examine the intracellular distribution of the components, we performed an aqueous two-phase partitioning experiment and found that they show three different patterns of distribution. OsRac1 localized in the plasma membrane and endomembrane fractions. Hop/Sti1a, Hsp70, and RACK1A were dispersed in the cytosol, endomembrane, and plasma membrane fractions. In contrast, Hsp90, SGT1, RAR1, and OsMPK6 were restricted mainly to the cytosol fraction, although a small proportion of Hsp90 partitioned to the plasma membrane fraction (Fig. 2C).

Next, we compared the intracellular transport system of OsCERK1 with that of Pit in rice protoplasts. We have previously revealed that OsCERK1 is sensitive to brefeldin A (BFA), an inhibitor of anterograde endoplasmic reticulum–Golgi transport, and is transported by a small GTPase Sar1-dependent vesicle trafficking pathway (Chen et al. 2010a; Takeuchi et al. 2000) (Fig. 2D). In contrast, Pit is a palmitoylated protein and localizes at the plasma membrane in rice protoplasts (Kawano et al. 2014a), and here we revealed that Pit is insensitive to BFA (Fig. 2D), indicating that OsCERK1 and Pit employ different intracellular transport pathways to reach the plasma membrane.

Monitoring the OsRac1 complex during OsCERK1-triggered immunity

To monitor the time course of OsRac1 activation after treatment with the fungal PAMP chitin, we employed a GST-PAK CRIB pull-down assay. This method exploits the Cdc42/Rac interactive binding (CRIB) domain of the Rac effector PAK1 (PAK CRIB), which shows a high affinity only for the active GTP-bound form of Rac, and not for the inactive GDP-bound form. This feature provides a useful tool to monitor the activation state of OsRac1 *in vivo* (Kawano et al. 2010a; Sander et al. 1998). As shown in Fig. 3A, a constitutively active mutant of OsRac1 (CA-OsRac1) specifically bound to PAK CRIB but a dominant-negative mutant (DN-OsRac1) did not, indicating that PAK CRIB should efficiently isolate the active GTP-bound form of OsRac1 from the crude cell lysate of suspension cells. Next, therefore, we prepared rice suspension cells expressing *myc-OsRac1 WT* to monitor the OsRac1 activation state after chitin treatment. A pull-down assay revealed statistically significant OsRac1 activation, beginning by 10 min after chitin treatment and lasting until at least 60 min (Fig. 3B). We investigated the dynamics of the OsRac1 complex by gel filtration and found that OsRac1 was divided into two groups: the high molecular weight OsRac1 fractions (HOR) (fractions 23–25; about 300 kDa) and the low molecular weight OsRac1 fractions (LOR) (fractions 29–31; about 50 kDa) (Fig. 3C). Intriguingly, a shift of WT OsRac1 from LOR to HOR was observed after a 10-min chitin treatment. We compared activation levels of OsRac1 between LOR and HOR using a GST-PAK CRIB pull-down assay. In the absence of chitin, total OsRac1 was distributed predominantly in LOR and gradually moved to HOR after chitin treatment (Fig. 3D, lower panel). Concomitantly, the active GTP form of OsRac1 was increased in HOR (Fig. 3D, higher panel), implying that activation of OsRac1 promotes the shift to HOR. To test this

hypothesis, we carried out a gel filtration assay using rice suspension cells expressing CA-OsRac1 and DN-OsRac1 (Fig. 3E). CA-OsRac1 was distributed exclusively in HOR, while DN-OsRac1 existed mainly in LOR. Next, we measured the amount of OsRac1 in the OsCERK1 complex after chitin treatment and found that chitin treatment induced the dissociation of OsRac1 from OsCERK1, but there were no obvious changes in the other components (Fig. 3F).

Monitoring the OsRac1 complex during Pit-triggered immunity

The active form of Pit activates OsRac1, and this activation seems to be critical for the induction of disease resistance to rice blast fungus (Kawano et al. 2010a; Wang et al. 2018). To examine the dynamics of the Pit complex, we generated rice suspension cells expressing *myc-OsRac1 WT* and either *Pit WT-FLAG* or *Pit D485V-FLAG*, which is a constitutively active mutant and triggers OsRac1 activation and cell death without fungus infection, under control of an estradiol-inducible promoter. We first checked the induction of *Pit D485V-FLAG* by estradiol at the RNA and protein levels (Fig. 4A). *Pit D485V-FLAG* mRNA was detected by RT-PCR after 1 h of estradiol treatment and gradually increased until 16 h. Correspondingly, a very faint band of Pit D485V-FLAG protein was observed 4 h after estradiol treatment began, and th protein had accumulated by 8 h. To analyze OsRac1 activation by Pit, we performed GST-pull down using GST-PAK CRIB (Fig. 4B). Induction of Pit D485V-FLAG by estradiol triggered activation of OsRac1; in contrast, induction of Pit WT-FLAG did not activate OsRac1 (Fig. 4B). Consistent with this, the transcript level of the defense gene *PAL1* in the Pit D485V cell line increased upon estradiol treatment (Fig. 4C). Similar to OsRac1 dynamics after chitin treatment, the ratio of HOR to LOR after the addition of estradiol was higher than that before the estradiol

258 treatment, suggesting that OsRac1 shifts from LOR to HOR as a consequence of the
259 expression of *Pit D485V* (Fig. 4D). Next, we tested whether chitin treatment affects
260 OsRac1–Pit interaction and found that OsRac1 was dissociated from Pit by the addition
261 of chitin (Fig. 4E), implying that there is crosstalk between OsCERK1 signaling and Pit
262 signaling.
263
264 **Hsp90 is an essential component of Pit-dependent immunity**
265 Since Hsp90 is critical for stabilizing several NLR proteins (Hubert et al. 2003; Kadota
266 and Shirasu 2012; Takahashi et al. 2003), its roles in ETI have been determined using
267 an Hsp90-specific inhibitor, geldanamycin (GDA). To clarify the role of Hsp90 in Pit-
268 induced defense responses, we tested the effect of GDA on Pit D485V-induced cell
269 death and ROS production in *Nicotiana benthamiana*. Overexpression of the
270 constitutively active mutant Pit D485V triggered cell death and ROS production, but this
271 effect was suppressed by the co-infiltration of GDA (Fig. 5A) and the knockdown of
272 endogenous *NbHsp90* by virus-induced gene silencing (Fig. 5B). Consistent with these
273 observations, *PAL1* induction by Pit D485V-FLAG was attenuated by GDA treatment in
274 rice suspension cells (Fig. 5C), indicating that proper Hsp90 activity is required for Pit-
275 induced immunity.
276 Finally, we monitored the localization of Pit in the presence of GDA in rice protoplasts.
277 As we have reported previously, Pit WT-Venus was localized in the plasma membrane,
278 but the addition of GDA abolished this plasma membrane localization of Pit WT and it
279 accumulated instead in the cytosol (Fig. 5D). We could not observe a fluorescent signal
280 of the constitutively active mutant Pit D485V-Venus in the absence of GDA, probably
281 due to cell death. Interestingly, a clear fluorescent signal of Pit D485V-Venus was

detected at the perinuclear region in the presence of GDA. This result implies that Hsp90 contributes to he maturation and/or proper plasma membrane localization of Pit and that it is indispensable for Pit's function.

Discussion

OsRac1 is a component of two distinct receptor complexes

OsRac1 is one of the critical regulators in rice immunity, working with two different types of immune receptors, the PRR OsCERK1 and the NLR Pit (Akamatsu et al. 2013; Kawano et al. 2010a; Wang et al. 2018). Consistent with this, we here showed that OsRac1 was associated with both OsCERK1 and Pit but formed two distinct receptor complexes (Fig. 1 and 2). It appears that OsRac1 does not interact directly with OsCERK1 but requires a mediator protein, Hop/Sti1, to bind to OsCERK1 (Chen et al. 2010a). In contrast, OsRac1 associates directly with the NB-ARC domain of Pit (Kawano et al. 2010a). In general, PTI and ETI employ common signaling pathways such as ROS and the MAPK cascade, but immune responses by ETI are more robust and prolonged than those by PTI (Tsuda and Katagiri 2010). OsRac1 may be one of the common key machineries that control both PTI and ETI in rice. OsRac1 regulates ROS production in PTI and ETI, possibly through direct interaction with the NADPH oxidases RbohB/H (Kawasaki et al. 1999; Kosami et al. 2014; Nagano et al. 2016; Wong et al. 2007). OsRac1 forms a complex with and controls OsMPK6 at the protein level (Lieberherr et al. 2005). Further studies are needed to elucidate how OsRac1 contributes to PTI and ETI in a mechanistically different manner.

In this study, we revealed that although both OsCERK1 and Pit were localized in the plasma membrane (Fig. 2D), they utilize different transport systems to anchor

306 themselves to the plasma membrane. We previously found that cysteine 97 and 98 in
307 the N-terminal CC region of Pit are palmitoylation sites that play critical roles in its
308 membrane localization and interaction with OsRac1 (Kawano et al. 2014a).
309 Palmitoylation, also known as S-acylation, is the reversible post-translational addition of
310 fatty acids to proteins and serves to target proteins to specific membrane compartments
311 and/or microdomains (Hemsley 2015). OsCERK1 depends on COPII-mediated ER-to-
312 Golgi traffic and on the *trans*-Golgi network for its transport to the plasma membrane (Fig.
313 2D) (Akamatsu et al. 2013; Chen et al. 2010a). Our previous BiFC analyses imply that
314 OsRac1 is associated with OsCERK1 and Pit in different places: OsRac1 forms a
315 complex with OsCERK1 through Hop/Sti1 possibly in the ER (Chen et al. 2010a) and
316 with Pit at the plasma membrane (Kawano et al. 2014a), supporting our new observation
317 that OsRac1 participates in distinct OsCERK1- and Pit-containing immune receptor
318 complexes (Fig. 2).
319
320 **OsRac1 assembles into large protein complexes during PTI and ETI**
321 Gel filtration and pull-down assay using GST-PAK CRIB revealed that the activation of
322 OsCERK1 and Pit led in turn to OsRac1 activation, which induced a shift of OsRac1 from
323 the LOR to the HOR, suggesting that OsRac1 activation by OsCERK1 and Pit activation
324 assembles in the large protein complexes. OsRac1 belongs to the Rac/Rop family of
325 small GTPases, which function as a molecular switch by cycling between GDP-bound
326 inactive and GTP-bound active forms in cells (Kawano et al. 2014b). The active GTP-
327 bound form of Rac/Rop binds to downstream target proteins to control various cellular
328 events (Kawano et al. 2014b). Until now, we have identified various direct downstream
329 target proteins of OsRac1, including the NADPH oxidases RbohB/H (Kosami et al. 2014;

Nagano et al. 2016; Wong et al. 2007), the lignin biosynthesis key enzyme cinnamoyl-CoA reductase (Kawasaki et al. 2006), the co-chaperones Hop/Sti1, and the scaffold protein RACK1 (Nakashima et al. 2008). The direct binding of OsRac1 to these downstream target proteins probably causes the shift of OsRac1 from the LOR to the HOR. We previously proposed that the OsCERK1–OsRacGEF1–OsRac1 module is one of the key components in chitin signaling in rice (Akamatsu et al. 2013). Here, we observed that the majority of OsRac1 existed in the LOR in the absence of chitin, and we found no obvious increment of OsRac1 protein in the OsCERK1 complex after chitin treatment, implying that the association of OsRac1 with OsRacGEF1 in the OsCERK1 complex is transient.

Roles of chaperones and co-chaperones in plant immunity

Here, we revealed that both OsCERK1 and Pit are also associated with the core chaperones Hsp90 and Hsp70 and the co-chaperone Hop/Sti1, and that SGT1 is a specific component of the Pit complex (Fig. 2A and 2B). We previously found that Hsp90 and Hop/Sti1 directly bind to OsCERK1 at the endoplasmic reticulum and contribute to the maturation of OsCERK1 and its transport to the plasma membrane (Chen et al. 2010a). Interactions between Hsp90 and various NLR proteins including RPM1, N, MLA1, MLA6, and Bs2 have been reported, and the LRR domain is likely an important site for NLR protein binding to Hsp90'? (Bieri et al. 2004; Hubert et al. 2003; Leister et al. 2005; Liu et al. 2004). One of the major roles for the Hsp90–SGT1–RAR1 complex is apparently to stabilize NLR proteins. GDA treatment or knockdown or knockout of *Hsp90*, *SGT1*, and *RAR1* compromises the plant's disease resistance to pathogens and reduces the levels of NLR proteins (Kadota et al. 2010). The complex presumably controls the

active/inactive state of NLR proteins. The pepper NLR protein Bs2 an intramolecular interaction between NB and LRR domains and this intramolecular interaction_that was abolished' by silencing *SGT1* (Leister et al. 2005), implying that SGT1 participates in the intramolecular interactions within NLR proteins. In this study, we revealed that the attenuation of Hsp90 expression or function compromised Pit-induced immune responses. Moreover, GDA treatment perturbed the plasma membrane localization of Pit (Fig. 5D). Taken together, these results suggest that the proper function of Pit requires the correct maturation of Pit by Hsp90. Further research is necessary to understand how their chaperones and co-chaperones orchestrate OsCERK1 and Pit.

Materials and Methods

Plasmid constructs

The cDNAs of *Pit*, *OsCERK1*, and *OsRac1* were described previously (Chen et al. 2010a; Kawano et al. 2010a). They were transferred into various vectors, depending on the experiment. These included pBI221-Vn-Gateway, pBI221-Gateway-Vc (provided by Dr. Seiji Takayama, University of Tokyo), and 35S-Gateway-Venus/GFP. We generated three pZH2B vectors containing the *Ubiquitin* promoter (*Ubq*Pro)-*4×myc-OsRac1 wild type (WT)-NOS* terminator (*NOS*Ter)-*Ubq*Pro-*OsCERK1-3×FLAG-Nos*Ter (Fig. 2A), *Ubq*Pro-*4×myc-OsRac1 WT-NOS*Ter-*Ubq*Pro-Pit WT-3*×FLAG-Nos*Ter (Fig. 2B), and *Ubq*Pro-*4×myc-OsRac1 WT-NOS*Ter-*Ubq*Pro-*OsCERK1-3×FLAG-Nos*Ter-*Ubq*Pro-Pit*×FLAG-Nos*Ter (Fig. 1A) by multiple steps of PCR, subcloning, and enzymatic digestion. We also produced two estradiol-inducible vectors pER8-*Pit WT* and *D485V-3×FLAG* with *Ubq*Pro-*4×myc-OsRac1-Nos*Ter (Fig. 4) (pER8 was provided by Dr. Nam-Hai Chua, Rockefeller University). pGPVX:Hsp90 (10-186) was generated using pGPVX:Hsp90 (10-186) vector (provided by Dr. Ken-Ichiro Taoka, Yokohama City University) containing the backbone of pGreen (Hellens et al. 2000), 35S promotor and PVX region of piX.erG3 (Tamai and Meshi 2001), and Hsp90 (10-186) (Lu et al. 2003).

Transgenic plants

Rice (*Oryza sativa* L. cv. Kinmaze) was used as the wild type and parental cultivar for the transgenic studies. Transgenic rice plants were generated using *Agrobacterium*-mediated transformation of rice calli (Hiei et al. 1994), and hygromycin-resistant plants were regenerated from transformed callus.

388

389 **Immunoprecipitation assay**

390 For co-IP assay, 500 mgof rice cultured suspension cells frozen in liquid nitrogen or rice
391 leaf blade samples were homogenized using a mortar with 1 ml of protein extraction
392 buffer [50 mM Tris, pH 7.5, 2 mM EDTA, 150 mM NaCl, 5 mM $MgCl_2$, 10% glycerol, 0.8%
393 (w/v) Triton X-100, 1× protease inhibitor cocktail, and phosphatase inhibitor cocktail 1
394 and 2 (Sigma)]. After a 20-min incubation on ice, the homogenized samples were
395 centrifuged at 20,000 × *g* for 20 min, and the resultant supernatants were collected.
396 Using the BCA Protein Assay Reagent (Pierce), the protein concentration of the
397 supernatants was measured and adjusted to 5 mg/ml protein with the protein extraction
398 buffer. For co-IP of Myc-tagged and HA-tagged proteins, the µMACS c-myc Isolation Kit
399 and µMACS HA Isolation Kit (Miltenyi Biotec) were used according to the instructions
400 provided. For co-IP of FLAG-tag proteins, Immunoprecipitation Kit-Dynabeads protein G
401 (Invitrogen) and Anti-FLAG M2 Monoclonal Antibody (Sigma-Aldrich) were used
402 according to the instructions provided.

403

404 **BiFC assay**

405 For use in BiFC experiments, *OsCERK1*, *Pit* and *OsRac1, Hop/Sti1a,* and *OsFLS2* were
406 cloned into BiFC vectors, which were then purified using the Purelink Plasmid Midiprep
407 Kit (Invitrogen) and introduced into rice protoplasts as described previously (Kawano et
408 al. 2014a; Wong et al. 2018). The mCherry expression plasmid was introduced
409 simultaneously as a marker for transformed cells. BiFC images were acquired using a
410 TCS SP5 confocal microscope (Leica).

411

412 **VIAFM observation**

413 *Pit* and *OsCERK1* were cloned into the *p35S-Gateway-mEGFP* and *-mCherry* vectors,
414 respectively, for C-terminal fusion using LR reactions (Thermo Fisher Scientific). Rice
415 protoplasts were transformed with these vectors as described previously (Wong et al.
416 2018). Ten to twelve hours after transformation, the cells were placed on a cover glass
417 (25 × 60 mm, NO.1; Matsunami) and then covered with another cover glass (25 × 40
418 mm, NO.1; Matsunami) thinly coated with low gelling temperature agarose (Sigma, cat.
419 no. A9414). VIAFM images were acquired using an Olympus TIRF system based on an
420 Olympus IX81 equipped with an APON 60XO TIRF (N.A.: 1.49). mEGFP and mCherry
421 were excited with 488- and 561-nm lasers, respectively.
422
423 **Subcellular localization in rice protoplasts**
424 Venus was fused to either the C or the N terminus of Pit using the Gateway system
425 (Invitrogen). The Pit-Venus, mCherry, and Cerulean-NLS constructs were controlled by
426 the CaMV 35S promoter. Protoplast isolation from rice Oc suspension cultures and
427 protoplast transformations were performed as described (Wong et al. 2018). Some of the
428 transfected cells were treated with BFA (50 μg/ml: Sigma) and GDA (10 μM: Sigma).
429 After incubation for 16 h at 30°C, the protoplasts were observed with a Leica TCS-SP5
430 microscope.
431
432 **Gel filtration**
433 One hundred fifty milligrams of rice cell culture was ground in liquid nitrogen and
434 extracted in 1 ml of protein extraction buffer for 20 min at 4°C. The extracts were
435 centrifuged at 20,000 × *g* for 20 min at 4°C, and the supernatant was filtered through a

436 0.22-µm filter (Millipore). The filtrate was applied to a Superdex 200 column (GE
437 Healthcare) attached to an AKTA Explorer system (GE Healthcare) using protein
438 extraction buffer as the running buffer. LMW and HMW Gel Filtration calibration kits (GE
439 Healthcare) were used to estimate the molecular weight of protein complexes. Fractions
440 of 0.5 ml each were collected and 45-µl aliquots were concentrated by TCA/acetone
441 precipitation. The precipitate was dissolved in 15 µl of SDS-PAGE sample buffer and
442 treated for 20 min at 60°C. These samples were subjected to SDS-PAGE and
443 immunoblot analysis.
444
445 **Pull-down assay using PAK CRIB**
446 Purified GST-PAK CRIB was prepared according to a previous method (Kawano et al.
447 2010a). Rice cell cultures were ground in liquid nitrogen and extracted in 1 ml of protein
448 extraction buffer for 20 min at 4°C. The extracts were centrifuged at 20,000 × *g* for 20
449 min at 4°C, and the supernatant was collected. Protein content was determined by the
450 BCA assay reagent (Thermo Fisher Scientific), using bovine serum albumin (BSA) as a
451 standard. Three milligrams of the total protein samples were applied to 20 µg of GST-
452 PAK-CRIB glutathione Sepharose 4B for pulldown assays and rotated for 30 min at 4°C.
453 The Sepharose was washed three times in protein extraction buffer. Proteins that
454 remained bound to the Sepharose were eluted in 80 µl of SDS-PAGE sample buffer and
455 treated for 20 min at 60°C. These samples were subjected to SDS-PAGE, immunoblot
456 analysis, and Coomassie staining.
457
458 **Preparation of membrane fractions**

Rice cell cultures were harvested 3 days after subculture and homogenized in homogenizing medium [50 mM MOPS/KOH, pH 7.6, 5 mM EGTA, 5 mM EDTA, 0.5 M D-sorbitol, 1.5% (w/v) polyvinylpyrrolidone, 2 mM PMSF, 2.5 mM DTT]. The homogenate was filtered through Miracloth (Calbiochem), and the filtrate was centrifuged at 3,000 × *g* for 10 min at 4°C. The supernatant was collected and centrifuged at 170,000 × *g* for 35 min at 4°C to yield soluble (supernatant) and microsomal (pellet) protein fractions. A polyethylene glycol–dextran (6.4%, w/w) aqueous two-phase partitioning system (Fujiwara et al. 2009) was used to separate the plasma membrane (PM) and endomembranes (EMs). The microsomal pellets were resuspended in MS-suspension medium [10 mM potassium phosphate, pH 7.8, 300 mM sucrose] and subjected to two-phase partitioning. Both the upper phase (enriched for the PM) and the lower phase (enriched for the EMs) were partitioned three times with lower phase buffer and upper phase buffer, respectively. The PM and EM fractions were harvested by centrifugation at 170,000 × *g* for 35 min at 4°C, and resuspended in PM-suspension medium (10 mM MOPS/KOH, pH 7.3, 1 mM EGTA, 300 mM sucrose, 2 mM DTT). The protein content of the fractions was determined by the BCA assay reagent (Thermo Fisher Scientific), using BSA as a standard. These samples were subjected to SDS-PAGE and immunoblot analysis.

Immunoblotting

Sample proteins were separated by SDS-PAGE and electrotransferred onto an Immobilon-P membrane (Millipore) for immunoblot detection. The membrane was blocked for 1 h in Blocking One (Nacalai Tesque) for 30 min and incubated for 30 min with anti-Myc (Nacalai Tesque) or anti-RACK1A (Nakashima et al. 2008), anti-FLAG

(Sigma), anti-Hop/Sti1a (Chen et al. 2010a), anti-OsCEBiP (Kaku et al. 2006), anti-Hsp90 (Enzo Life Sciences), anti-SGT1 (Azevedo et al. 2002), anti-RAR1 (Thao et al. 2007), anti-OsMPK6 (Lieberherr et al. 2005), anti-tubulin (Calbiochem), anti-Bip (Cosmo Bio), and anti-OsPIP1s (Cosmo Bio) antibodies. After washing twice with TBST (0.05 M Tris, pH 7.6, 0.9% NaCl, 0.1% Triton X-100), the membranes were incubated for 2 h in Can Get Signal Solution 2 (Toyobo) with anti-rabbit or mouse IgG conjugated to horseradish peroxidase (GE Healthcare). After washing twice with TBST, chemical enhancement was performed using ECL PLUS Western blot detection reagents (GE Healthcare). The enhanced signals were detected by the LAS-4000 system (Fujifilm).

Agroinfiltration into *N. benthamiana* leaves

In some experiments, we generated *pGPVX:Hsp90* (10-186) vector and virus-induced gene silencing (VIGS) was done as described by Lu *et al.* (Lu et al. 2003). Agroinfiltration of *N. benthamiana* was performed as described previously (Kawano et al. 2010a). *Agrobacterium tumefaciens* strain GV3010, harboring the helper plasmid pSoup and binary plasmids carrying the cDNAs of Pit WT and mutants, was used to infiltrate leaves of 5-week-old *N. benthamiana* plants. We used the p19 silencing suppressor to enhance gene expression. Each *Agrobacterium* culture was resuspended in a buffer containing 10 mM $MgCl_2$, 10 mM MES, pH 5.6, and 150 μM acetosyringone, and incubated at 23°C for 2–3 h before infiltration. In some experiments, we added GDA at a final concentration of 10 μM to an *Agrobacterium* culture carrying pGWB2-*Pit D485V*. The plants were kept in a growth chamber at 23°C after agroinfiltration. To visualize hydrogen peroxide, a major endogenous ROS, *in situ*, the agroinfiltrated leaves were detached and incubated in 1 μg/ml DAB solution for 2–8 h, after which they were decolorized in boiling ethanol.

Photographs were taken at 7 days post-inoculation (dpi) for cell death at 3 dpi for ROS production.

Funding

This work was supported by the Chinese Academy of Sciences, Shanghai Institutes for Biological Sciences, Shanghai Center for Plant Stress Biology, CAS Center of Excellence for Molecular Plant Sciences, Strategic Priority Research Program of the Chinese Academy of Sciences (B) (XDB27040202), the Chinese Academy of Sciences Hundred Talents Program (173176001000162114), the National Natural Science Foundation of China (31572073 and 31772246), JSPS KAKENHI (26450055, 17K07668, and 20H02988), and the Ohara Foundation. K. K. was supported by the CAS President's International Fellowship Initiative (2019PB0056). A. A. was supported by a Grant-in-Aid for Early-Career Scientists (20K15426).

Disclosures

Conflicts of interest: No conflicts of interest declared

Acknowledgments

We thank the members of the Laboratory of Plant Molecular Genetics at NAIST, the Laboratory of Signal Transduction and Immunity at PSC, and the Plant Immune Design Group at Okayama University for invaluable support and discussions.

References

Akamatsu, A., Uno, K., Kato, M., Wong, H.L., Shimamoto, K. and Kawano, Y. (2015) New insights into the dimerization of small GTPase Rac/ROP guanine nucleotide exchange factors in rice. *Plant Signal Behav* 10: e1044702.

Akamatsu, A., Wong, H., Fujiwara, M., Okuda, J., Nishide, K., Uno, K., et al. (2013) An OsCEBiP/OsCERK1-OsRacGEF1-OsRac1 module is an essential component of chitin-induced rice immunity. *Cell Host Microbe* 13: 465-476.

Azevedo, C., Sadanandom, A., Kitagawa, K., Freialdenhoven, A., Shirasu, K. and Schulze-Lefert, P. (2002) The RAR1 interactor SGT1, an essential component of R gene-triggered disease resistance. *Science* 295: 2073-2076.

Berken, A. (2006) ROPs in the spotlight of plant signal transduction. *Cell Mol Life Sci* 63: 2446-2459.

Bieri, S., Mauch, S., Shen, Q.H., Peart, J., Devoto, A., Casais, C., et al. (2004) RAR1 positively controls steady state levels of barley MLA resistance proteins and enables sufficient MLA6 accumulation for effective resistance. *Plant Cell* 16: 3480-3495.

Chen, L., Hamada, S., Fujiwara, M., Zhu, T., Thao, N.P., Wong, H.L., et al. (2010a) The Hop/Sti1-Hsp90 chaperone complex facilitates the maturation and transport of a PAMP receptor in rice innate immunity. *Cell Host Microbe* 7: 185-196.

Chen, L., Shiotani, K., Togashi, T., Miki, D., Aoyama, M., Wong, H.L., et al. (2010b) Analysis of the Rac/Rop small GTPase family in rice: expression, subcellular localization and role in disease resistance. *Plant Cell Physiol* 51: 585-595.

Couto, D. and Zipfel, C. (2016) Regulation of pattern recognition receptor signalling in plants. *Nat Rev Immunol* 16: 537-552.

Cui, H., Tsuda, K. and Parker, J.E. (2015) Effector-triggered immunity: from pathogen perception to robust defense. *Annu Rev Plant Biol* 66: 487-511.

Dangl, J.L., Horvath, D.M. and Staskawicz, B.J. (2013) Pivoting the plant immune system from dissection to deployment. *Science* 341: 746-751.

Dodds, P.N. and Rathjen, J.P. (2010) Plant immunity: towards an integrated view of plant-pathogen interactions. *Nat Rev Genet* 11: 539-548.

Fujimoto, M., Arimura, S., Ueda, T., Takanashi, H., Hayashi, Y., Nakano, A., et al. (2010) Arabidopsis dynamin-related proteins DRP2B and DRP1A participate together in clathrin-coated vesicle formation during endocytosis. *Proc Natl Acad Sci U S A* 107: 6094-6099.

564 Fujiwara, M., Hamada, S., Hiratsuka, M., Fukao, Y., Kawasaki, T. and Shimamoto, K.
565 (2009) Proteome analysis of detergent-resistant membranes (DRMs) associated
566 with OsRac1-mediated innate immunity in rice. *Plant Cell Physiol* 50: 1191-1200.
567 Hellens, R.P., Edwards, E.A., Leyland, N.R., Bean, S. and Mullineaux, P.M. (2000)
568 pGreen: a versatile and flexible binary Ti vector for Agrobacterium-mediated plant
569 transformation. *Plant Mol Biol* 42: 819-832.
570 Hemsley, P.A. (2015) The importance of lipid modified proteins in plants. *New Phytol*
571 205: 476-489.
572 Hiei, Y., Ohta, S., Komari, T. and Kumashiro, T. (1994) Efficient transformation of rice
573 (Oryza sativa L.) mediated by Agrobacterium and sequence analysis of the
574 boundaries of the T-DNA. *Plant J* 6: 271-282.
575 Hubert, D.A., Tornero, P., Belkhadir, Y., Krishna, P., Takahashi, A., Shirasu, K., et al.
576 (2003) Cytosolic HSP90 associates with and modulates the Arabidopsis RPM1
577 disease resistance protein. *EMBO J* 22: 5679-5689.
578 Ishiguro, S., Watanabe, Y., Ito, N., Nonaka, H., Takeda, N., Sakai, T., et al. (2002)
579 SHEPHERD is the Arabidopsis GRP94 responsible for the formation of functional
580 CLAVATA proteins. *EMBO J* 21: 898-908.
581 Kadota, Y. and Shirasu, K. (2012) The HSP90 complex of plants. *Biochim Biophys Acta*
582 1823: 689-697.
583 Kadota, Y., Shirasu, K. and Guerois, R. (2010) NLR sensors meet at the SGT1-HSP90
584 crossroad. *Trends Biochem Sci* 35: 199-207.
585 Kaku, H., Nishizawa, Y., Ishii-Minami, N., Akimoto-Tomiyama, C., Dohmae, N., Takio, K.,
586 et al. (2006) Plant cells recognize chitin fragments for defense signaling through a
587 plasma membrane receptor. *Proc Natl Acad Sci U S A* 103: 11086-11091.
588 Kawano, Y., Akamatsu, A., Hayashi, K., Housen, Y., Okuda, J., Yao, A., et al. (2010a)
589 Activation of a Rac GTPase by the NLR family disease resistance protein Pit plays
590 a critical role in rice innate immunity. *Cell Host Microbe* 7: 362-375.
591 Kawano, Y., Chen, L. and Shimamoto, K. (2010b) The function of Rac small GTPase
592 and associated proteins in rice innate immunity. *Rice* 3: 112-121.
593 Kawano, Y., Fujiwara, T., Yao, A., Housen, Y., Hayashi, K. and Shimamoto, K. (2014a)
594 Palmitoylation-dependent membrane localization of the rice resistance protein pit
595 is critical for the activation of the small GTPase OsRac1. *J Biol Chem* 289: 19079-
596 19088.
597 Kawano, Y., Kaneko-Kawano, T. and Shimamoto, K. (2014b) Rho family GTPase-
598 dependent immunity in plants and animals. *Front in Plant Sci* 5: 522.

599 Kawano, Y. and Shimamoto, K. (2013) Early signaling network in rice PRR- and R-
600 mediated immunity. *Curr Opin Plant Biol* 16: 496–504.
601 Kawasaki, T., Henmi, K., Ono, E., Hatakeyama, S., Iwano, M., Satoh, H., et al. (1999)
602 The small GTP-binding protein Rac is a regulator of cell death in plants. *Proc Natl*
603 *Acad Sci U S A* 96: 10922-10926.
604 Kawasaki, T., Koita, H., Nakatsubo, T., Hasegawa, K., Wakabayashi, K., Takahashi, H.,
605 et al. (2006) Cinnamoyl-CoA reductase, a key enzyme in lignin biosynthesis, is an
606 effector of small GTPase Rac in defense signaling in rice. *Proc Natl Acad Sci U S*
607 *A* 103: 230-235.
608 Kim, S.H., Oikawa, T., Kyozuka, J., Wong, H.L., Umemura, K., Kishi-Kaboshi, M., et al.
609 (2012) The bHLH Rac immunity1 (RAI1) is activated by OsRac1 via OsMAPK3 and
610 OsMAPK6 in rice immunity. *Plant Cell Physiol* 53: 740-754.
611 Konopka, C.A. and Bednarek, S.Y. (2008) Variable-angle epifluorescence microscopy:
612 a new way to look at protein dynamics in the plant cell cortex. *Plant J* 53: 186-196.
613 Kosami, K., Ohki, I., Nagano, M., Furuita, K., Sugiki, T., Kawano, Y., et al. (2014) The
614 crystal structure of the plant small GTPase OsRac1 reveals its mode of binding to
615 NADPH oxidase. *J Biol Chem* 289: 28569-28578.
616 Leister, R.T., Dahlbeck, D., Day, B., Li, Y., Chesnokova, O. and Staskawicz, B.J. (2005)
617 Molecular genetic evidence for the role of SGT1 in the intramolecular
618 complementation of Bs2 protein activity in Nicotiana benthamiana. *Plant Cell* 17:
619 1268-1278.
620 Lieberherr, D., Thao, N.P., Nakashima, A., Umemura, K., Kawasaki, T. and Shimamoto,
621 K. (2005) A sphingolipid elicitor-inducible mitogen-activated protein kinase is
622 regulated by the small GTPase OsRac1 and heterotrimeric G-protein in rice. *Plant*
623 *Physiol* 138: 1644-1652.
624 Liu, Y., Burch-Smith, T., Schiff, M., Feng, S. and Dinesh-Kumar, S.P. (2004) Molecular
625 chaperone Hsp90 associates with resistance protein N and its signaling proteins
626 SGT1 and Rar1 to modulate an innate immune response in plants. *J Biol Chem*
627 279: 2101-2108.
628 Lu, R., Malcuit, I., Moffett, P., Ruiz, M.T., Peart, J., Wu, A.J., et al. (2003) High throughput
629 virus-induced gene silencing implicates heat shock protein 90 in plant disease
630 resistance. *EMBO J* 22: 5690-5699.
631 Monaghan, J. and Zipfel, C. (2012) Plant pattern recognition receptor complexes at the
632 plasma membrane. *Curr Opin Plant Biol* 15: 349-357.

N'gou, B.P.M., Ahn, H.-K., Ding, P. and Jones, J. (2020) Mutual Potentiation of Plant Immunity by Cell-surface and Intracellular Receptors. *bioRxiv* https://doi.org/10.1101/2020.04.10.034173.

Nagano, M., Ishikawa, T., Fujiwara, M., Fukao, Y., Kawano, Y., Kawai-Yamada, M., et al. (2016) Plasma Membrane Microdomains Are Essential for Rac1-RbohB/H-Mediated Immunity in Rice. *Plant Cell* 28: 1966-1983.

Nakashima, A., Chen, L., Thao, N.P., Fujiwara, M., Wong, H.L., Kuwano, M., et al. (2008) RACK1 functions in rice innate immunity by interacting with the Rac1 immune complex. *Plant Cell* 20: 2265-2279.

Nibau, C., Wu, H.M. and Cheung, A.Y. (2006) RAC/ROP GTPases: 'hubs' for signal integration and diversification in plants. *Trends Plant Sci* 11: 309-315.

Ono, E., Wong, H.L., Kawasaki, T., Hasegawa, M., Kodama, O. and Shimamoto, K. (2001) Essential role of the small GTPase Rac in disease resistance of rice. *Proc Natl Acad Sci U S A* 98: 759-764.

Pearl, L.H. and Prodromou, C. (2006) Structure and mechanism of the Hsp90 molecular chaperone machinery. *Annu Rev Biochem* 75: 271-294.

Peng, Y., van Wersch, R. and Zhang, Y. (2018) Convergent and Divergent Signaling in PAMP-Triggered Immunity and Effector-Triggered Immunity. *Mol Plant Microbe Interact* 31: 403-409.

Qi, Y., Tsuda, K., Glazebrook, J. and Katagiri, F. (2011) Physical association of pattern-triggered immunity (PTI) and effector-triggered immunity (ETI) immune receptors in Arabidopsis. *Mol Plant Pathol* 12: 702-708.

Sander, E.E., van Delft, S., ten Klooster, J.P., Reid, T., van der Kammen, R.A., Michiels, F., et al. (1998) Matrix-dependent Tiam1/Rac signaling in epithelial cells promotes either cell-cell adhesion or cell migration and is regulated by phosphatidylinositol 3-kinase. *J Cell Biol* 143: 1385-1398.

Shirasu, K., Lahaye, T., Tan, M.W., Zhou, F., Azevedo, C. and Schulze-Lefert, P. (1999) A novel class of eukaryotic zinc-binding proteins is required for disease resistance signaling in barley and development in C. elegans. *Cell* 99: 355-366.

Takahashi, A., Casais, C., Ichimura, K. and Shirasu, K. (2003) HSP90 interacts with RAR1 and SGT1 and is essential for RPS2-mediated disease resistance in Arabidopsis. *Proc Natl Acad Sci U S A* 100: 11777-11782.

Takeuchi, M., Ueda, T., Sato, K., Abe, H., Nagata, T. and Nakano, A. (2000) A dominant negative mutant of sar1 GTPase inhibits protein transport from the endoplasmic reticulum to the Golgi apparatus in tobacco and Arabidopsis cultured cells. *Plant J* 23: 517-525.

669 Tamai, A. and Meshi, T. (2001) Cell-to-cell movement of Potato virus X: the role of p12
670 and p8 encoded by the second and third open reading frames of the triple gene
671 block. *Mol Plant Microbe Interact* 14: 1158-1167.
672 Tao, Y., Xie, Z., Chen, W., Glazebrook, J., Chang, H.S., Han, B., et al. (2003)
673 Quantitative nature of Arabidopsis responses during compatible and incompatible
674 interactions with the bacterial pathogen Pseudomonas syringae. *Plant Cell* 15:
675 317-330.
676 Thao, N.P., Chen, L., Nakashima, A., Hara, S., Umemura, K., Takahashi, A., et al. (2007)
677 RAR1 and HSP90 form a complex with Rac/Rop GTPase and function in innate-
678 immune responses in rice. *Plant Cell* 19: 4035-4045.
679 Thomma, B.P., Nurnberger, T. and Joosten, M.H. (2011) Of PAMPs and effectors: the
680 blurred PTI-ETI dichotomy. *Plant Cell* 23: 4-15.
681 Tsuda, K. and Katagiri, F. (2010) Comparing signaling mechanisms engaged in pattern-
682 triggered and effector-triggered immunity. *Curr Opin Plant Biol* 13: 459-465.
683 Tsuda, K., Mine, A., Bethke, G., Igarashi, D., Botanga, C.J., Tsuda, Y., et al. (2013) Dual
684 regulation of gene expression mediated by extended MAPK activation and salicylic
685 acid contributes to robust innate immunity in Arabidopsis thaliana. *PLoS genetics*
686 9: e1004015.
687 Wang, Q., Li, Y., Ishikawa, K., Kosami, K.I., Uno, K., Nagawa, S., et al. (2018) Resistance
688 protein Pit interacts with the GEF OsSPK1 to activate OsRac1 and trigger rice
689 immunity. *Proc Natl Acad Sci U S A* 115: E11551-E11560.
690 Wong, H.L., Akamatsu, A., Wang, Q., Higuchi, M., Matsuda, T., Okuda, J., et al. (2018)
691 In vivo monitoring of plant small GTPase activation using a Forster resonance
692 energy transfer biosensor. *Plant Methods* 14: 56.
693 Wong, H.L., Pinontoan, R., Hayashi, K., Tabata, R., Yaeno, T., Hasegawa, K., et al.
694 (2007) Regulation of rice NADPH oxidase by binding of Rac GTPase to its N-
695 terminal extension. *Plant Cell* 19: 4022-4034.
696 Yalovsky, S., Bloch, D., Sorek, N. and Kost, B. (2008) Regulation of membrane trafficking,
697 cytoskeleton dynamics, and cell polarity by ROP/RAC GTPases. *Plant Physiol* 147:
698 1527-1543.
699 Yuan, M., Jian, Z., Bi, G., Nomura, K., Liu, M., He, S.Y., et al. (2020) Pattern-recognition
700 receptors are required for NLR-mediated plant immunity. *bioRxiv*
701 https://doi.org/10.1101/2020.04.10.031294.

702

Legends to Figures

Fig. 1 OsRac1 forms two distinct immune receptor complexes

(A) *In vivo* interaction between the chitin receptor OsCERK1 and the NLR protein Pit. Co-IP was performed using an anti-HA and anti-FLAG antibodies, and the proteins were detected by immunoblot with the indicated antibodies. (B) BiFC assay between OsCERK1 and Pit. Expression of the indicated genes was driven by the CaMV 35S promoter. The graph shows the percentage of BiFC positive cells. Scale bars, 5 μm. (C) Representative VIAFM images of rice protoplasts expressing Pit-WT-mEGFP and OsCERK1-mCherry. Left, center, and right panels are GFP, mCherry, and merged images, respectively. Scale bar, 5 μm.

Fig. 2 Components of OsCERK1- and Pit-containing immune complexes

(A, B) Co-IP of (A) OsCERK1- and (B) Pit-containing immune complexes. Co-IP was performed using anti-FLAG antibody, and the proteins were detected by immunoblot with the indicated antibodies. (C) Distribution of defense-related proteins. An aqueous two-phase partitioning experiment was performed and the proteins were detected by immunoblot with the indicated antibodies. (D) Localization of OsCERK1 and Pit in rice protoplasts in the presence of BFA. OsCERK1-GFP or Pit1-Venus was co-transfected with mCherry. Sixteen hours after BFA treatment, the transfected cells were observed under a microscope. Scale bars, 5 μm.

Fig. 3 Active OsRac1 forms a large immune complex after chitin treatment

(A) GST-PAK CRIB pull-down assay using rice suspension cells expressing a dominant-negative mutant of *OsRac1* (*DN-OsRac1*) and a constitutively active mutant of *OsRac1* (*CA-OsRac1*). The band of GTP•OsRac1 indicates the amount of the active form of OsRac1. (B) Monitoring OsRac1 activation after chitin treatment. Rice suspension cells expressing myc-OsRac1 WT were treated with chitin and the resultant cell lysates were subjected to GST-PAK CRIB pull-down assay to detect OsRac1 activation. The graph indicates the band intensity analyzed by ImageJ software. Error bars indicate the SD. Different letters above bars indicate a significant difference determined by Student's *t*-test ($P < 0.05$). (C) Gel filtration fractions of protein extracts from rice suspension cells expressing *OsRac1 WT* before and after chitin treatment (upper and lower panels) were subjected to immunoblot analyses using an anti-Myc antibody. Fraction numbers and relative molecular masses (kDa) are indicated at the top and bottom, respectively. (D) Combined high-molecular-weight OsRac1 fractions (HOR) (fractions 23–25 in (C)) or low-molecular-weight OsRac1 fractions (LOR) (fractions 29–31) were applied to GST-PAK CRIB pull-down assay to monitor OsRac1 activation. (E) Gel filtration fractions of protein extracts from rice suspension cells expressing *OsRac1 WT*, *CA*, *and DN*. Fraction numbers and relative molecular masses (kD) are indicated at the top and bottom, respectively. (F) Components of the OsCERK1 complex after chitin treatment. OsCERK1-FLAG was immunoprecipitated with an anti-FLAG antibody. The precipitates were immunoblotted with the indicated antibodies.

Fig. 4 Active-form Pit shifts OsRac1 to the larger immune complex

(A) Induction of constitutively active *Pit* (*Pit D485V*) mRNA and protein by estradiol treatment. (B) Expression of Pit D485V triggers OsRac1 activation. After the induction of Pit D485V by estradiol, we carried out a GST-PAK CRIB pull-down assay to detect OsRac1 activation. (C) Defense gene *PAL1* is induced by the expression of *Pit D485V*.

(D) Gel filtration fractions of protein extract from rice suspension cells expressing OsRac1 WT before and after Pit D485V induction. Fraction numbers and relative molecular masses (kD) are indicated at the top and bottom, respectively. (E) Interaction between Pit and OsRac1 after chitin treatment. After chitin treatment, Pit-FLAG was precipitated by an anti-FLAG antibody. The resultant precipitates were immunoblotted with anti-Myc antibody.

Fig. 5 Hsp90 contributes to Pit-induced immunity

(A) Suppression of Pit-triggered cell death and ROS production by the Hsp90 inhibitor GDA. In the presence or absence of GDA, Pit D485V-induced cell death (left image) and ROS (right image) were examined in *N. benthamiana* leaves. (B) Suppression of Pit D485V-induced cell death by virus-induced gene silencing (VIGS) of Hsp90. *N. benthamiana* plants were inoculated with pGPVX:GFP or pGPVX:Hsp90 (10-186), and three weeks later the upper leaves were infiltrated with a mixture of *Agrobacterium* cultures carrying pGWB2-Pit D485V transgenes. Cell death developed by 7 days after inoculation (upper panels). mRNA expression of *Hsp90* and the internal control *Actin* was detected by RT-PCR (lower panels). (C) Inhibition of *Pit D485V*-induced *PAL1* expression by treatment of with GDA. mRNA expression of *PAL1*, *Pit*, *OsRac1*, *Hsp90*, and *Actin* was detected by RT-PCR. (D) Localization of Pit-Venus in rice protoplasts in the presence of GDA. Pit-Venus was co-transfected with mCherry. Twelve hours after GDA treatment, the transfected cells were observed under a microscope. Scale bars, 5 μm.

775 **Table1 List of primers**

776

Primer name	Primer sequence
Myc-OsRac1 F	5'-AGCTTGGGCGACCTCACCTCTG-3'
Myc-OsRac1 R	5'-ACATCCTTATGTCTTGGAGGTTG-3'
OsCERK1-FLAG F	5'-CACCATGTTTAGTATTGGCAATAAAATAGG-3'
OsCERK1-FLAG R	5'-GCTGTTATCAACCACTTTGTA-3'
Pit-FLAG F	5'-GCCAGATGCCAGAACTGCTA-3'
Pit-FLAG R	5'-GCTGTTATCAACCACTTTGTA-3'
PAL1 F	5'-CTACCCGCTGATGAAGAAGC-3'
PAL1 R	5'-AACCTGCCACTCGTACCAAGTTTTGC-3'

777

778

779

780

781

782

783

Akamatsu et al., Figure 1

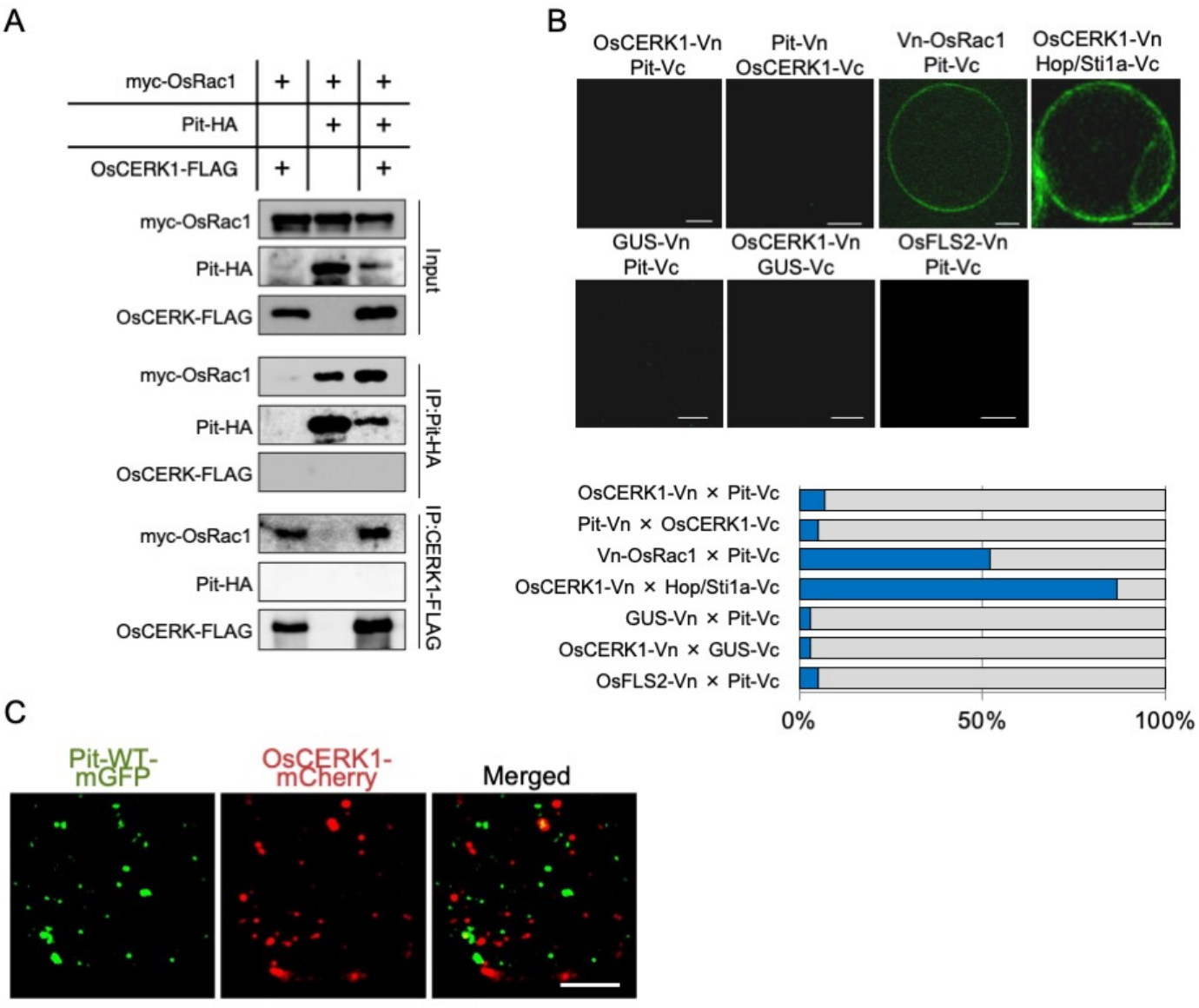

Fig. 1 OsRac1 forms two distinct immune receptor complexes

(A) *In vivo* interaction between the chitin receptor OsCERK1 and the NLR protein Pit. Co-IP was performed using an anti-HA and anti-FLAG antibodies, and the proteins were detected by immunoblot with the indicated antibodies. (B) BiFC assay between OsCERK1 and Pit. Expression of the indicated genes was driven by the CaMV 35S promoter. The graph shows the percentage of BiFC positive cells. Scale bars, 5 μm. (C) Representative VIAFM images of rice protoplasts expressing Pit-WT-mEGFP and OsCERK1-mCherry. Left, center, and right panels are GFP, mCherry, and merged images, respectively. Scale bar, 5 μm.

Akamatsu et al., Figure 2

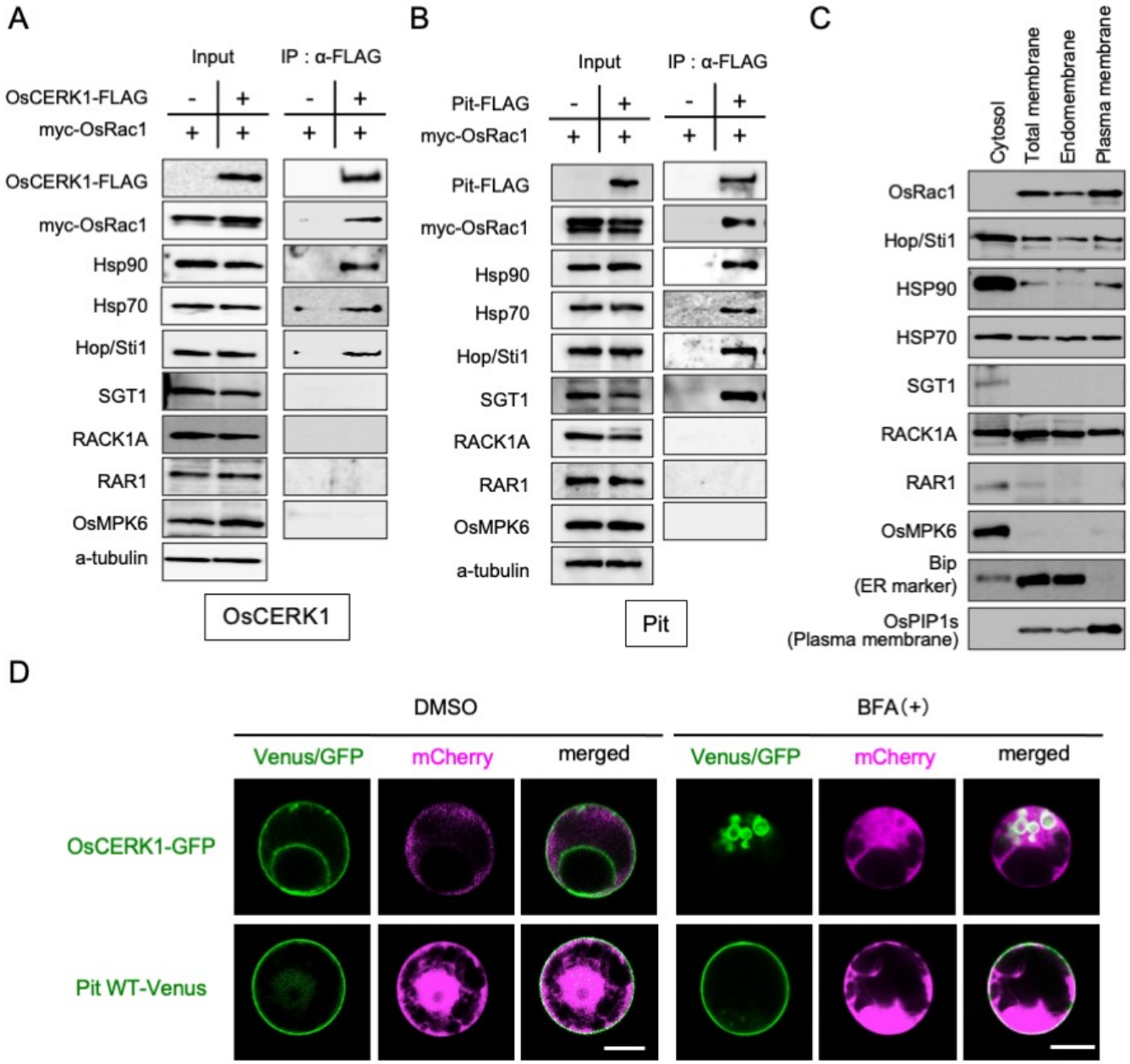

Fig. 2 Components of OsCERK1- and Pit-containing immune complexes

(A, B) Co-IP of (A) OsCERK1- and (B) Pit-containing immune complexes. Co-IP was performed using anti-FLAG antibody, and the proteins were detected by immunoblot with the indicated antibodies. (C) Distribution of defense-related proteins. An aqueous two-phase partitioning experiment was performed and the proteins were detected by immunoblot with the indicated antibodies. (D) Localization of OsCERK1 and Pit in rice protoplasts in the presence of BFA. OsCERK1-GFP or Pit1-Venus was co-transfected with mCherry. Sixteen hours after BFA treatment, the transfected cells were observed under a microscope. Scale bars, 5 μm.

Akamatsu et al., Figure 3

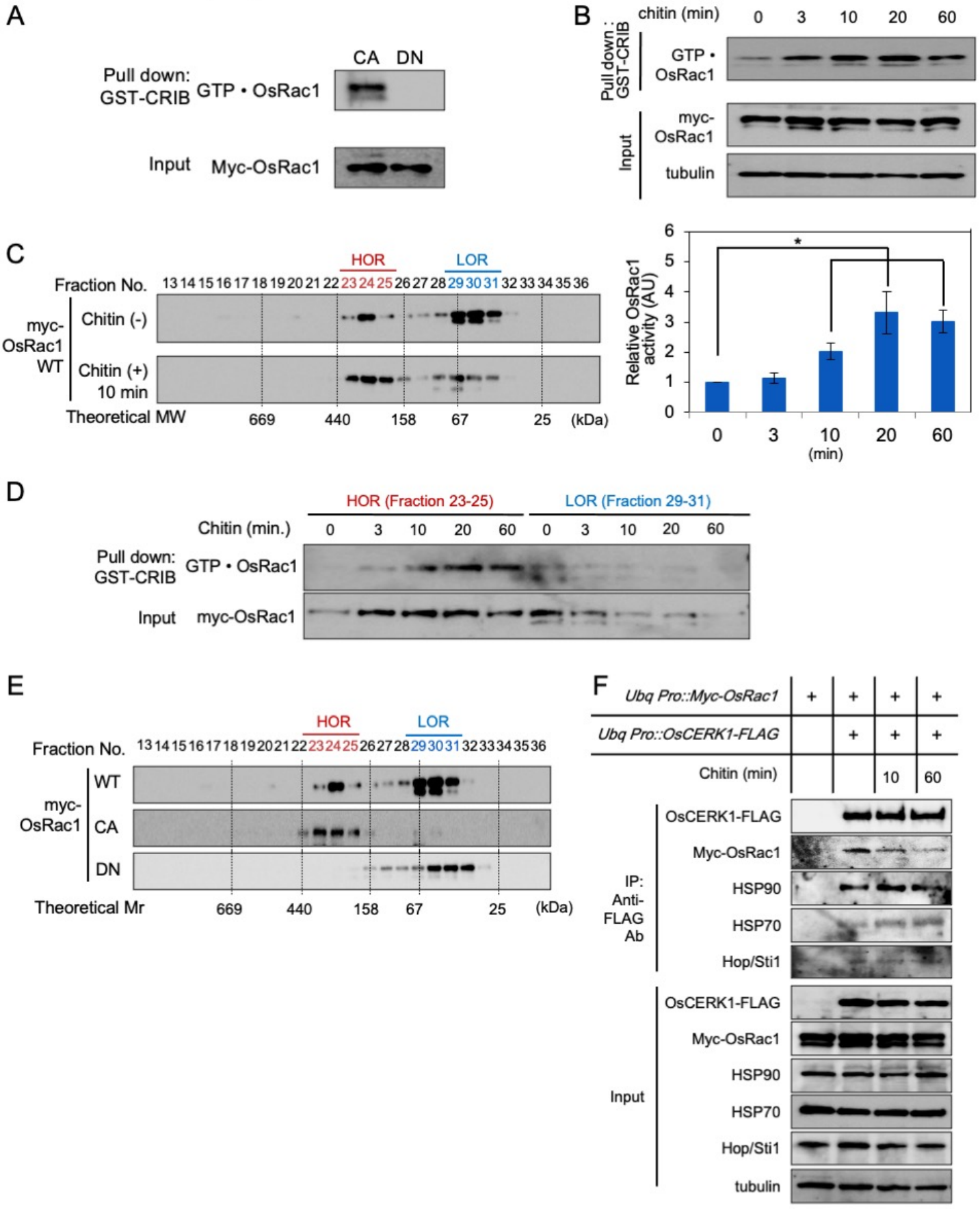

Fig. 3 Active OsRac1 forms a large immune complex after chitin treatment

(A) GST-PAK CRIB pull-down assay using rice suspension cells expressing a dominant-negative mutant of *OsRac1* (*DN-OsRac1*) and a constitutively active mutant of *OsRac1* (*CA-OsRac1*). The band of GTP•OsRac1 indicates the amount of the active form of OsRac1. (B) Monitoring OsRac1 activation after chitin treatment. Rice suspension cells expressing myc-OsRac1 WT were treated with chitin and the resultant cell lysates were subjected to GST-PAK CRIB pull-down assay to detect OsRac1 activation. The graph indicates the band intensity analyzed by ImageJ software. Error bars indicate the SD. Different letters above bars indicate a significant difference determined by Student's *t*-test ($P < 0.05$). (C) Gel filtration fractions of protein extracts from rice suspension cells expressing *OsRac1 WT* before and after chitin treatment (upper and lower panels) were subjected to immunoblot analyses using an anti-Myc antibody. Fraction numbers and relative molecular masses (kDa) are indicated at the top and bottom, respectively. (D) Combined high-molecular-weight OsRac1 fractions (HOR) (fractions 23–25 in (C)) or low-molecular-weight OsRac1 fractions (LOR) (fractions 29–31) were applied to GST-PAK CRIB pull-down assay to monitor OsRac1 activation. (E) Gel filtration fractions of protein extracts from rice suspension cells expressing *OsRac1 WT*, *CA*, *and DN*. Fraction numbers and relative_molecular masses (kD) are indicated at the top and bottom, respectively. (F) Components of the OsCERK1 complex after chitin treatment. OsCERK1-FLAG was immunoprecipitated with an anti-FLAG antibody. The precipitates were immunoblotted with the indicated antibodies.

Akamatsu et al., Figure 4

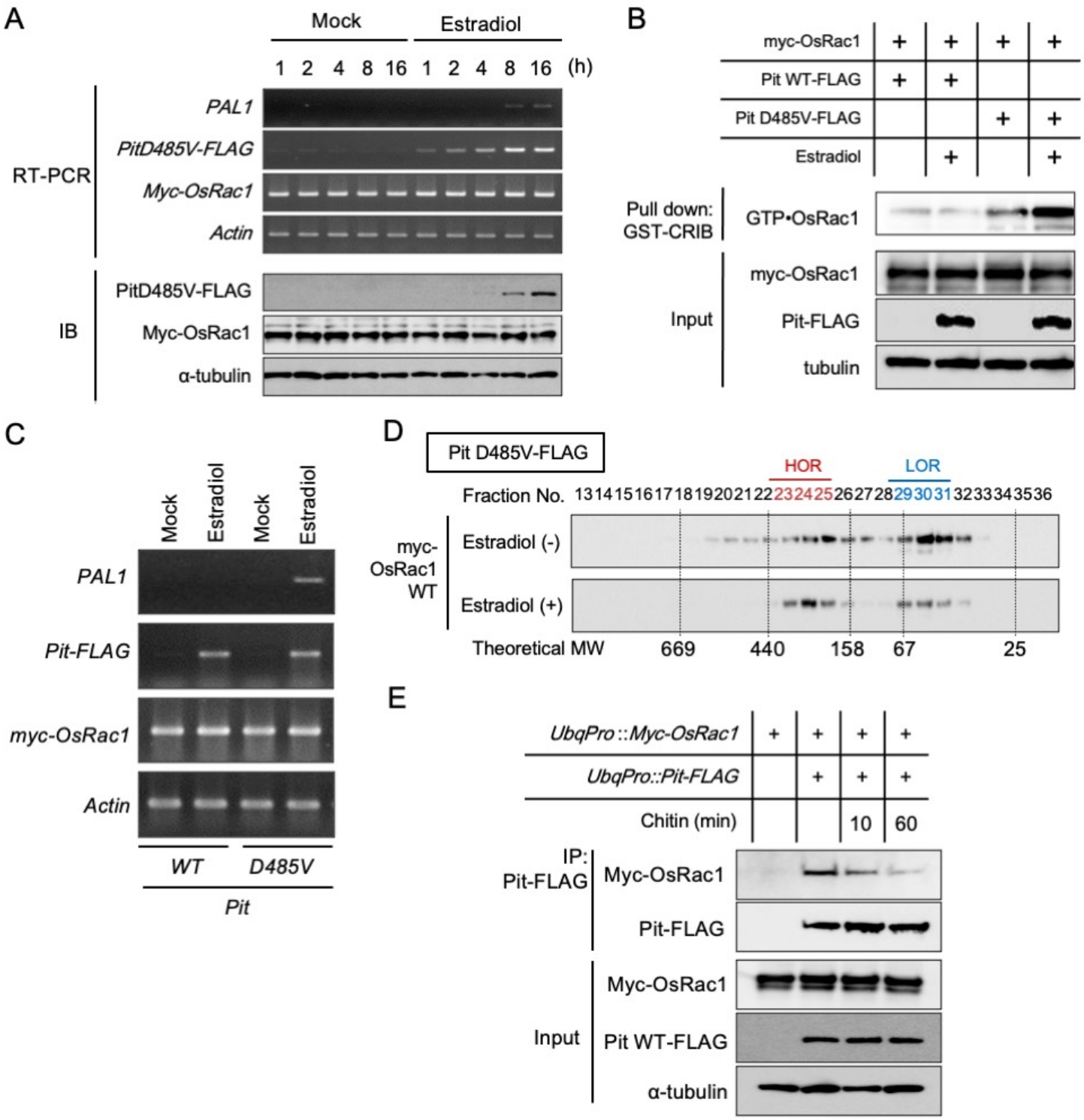

Fig. 4 Active-form Pit shifts OsRac1 to the larger immune complex

(A) Induction of constitutively active *Pit* (*Pit D485V*) mRNA and protein by estradiol treatment. (B) Expression of Pit D485V triggers OsRac1 activation. After the induction of Pit D485V by estradiol, we carried out a GST-PAK CRIB pull-down assay to detect OsRac1 activation. (C) Defense gene *PAL1* is induced by the expression of *Pit D485V*. (D) Gel filtration fractions of protein extract from rice suspension cells expressing OsRac1 WT before and after Pit D485V induction. Fraction numbers and relative molecular masses (kD) are indicated at the top and bottom, respectively. (E) Interaction between Pit and OsRac1 after chitin treatment. After chitin treatment, Pit-FLAG was precipitated by an anti-FLAG antibody. The resultant precipitates were immunoblotted with anti-Myc antibody.

Akamatsu et al., Figure 5

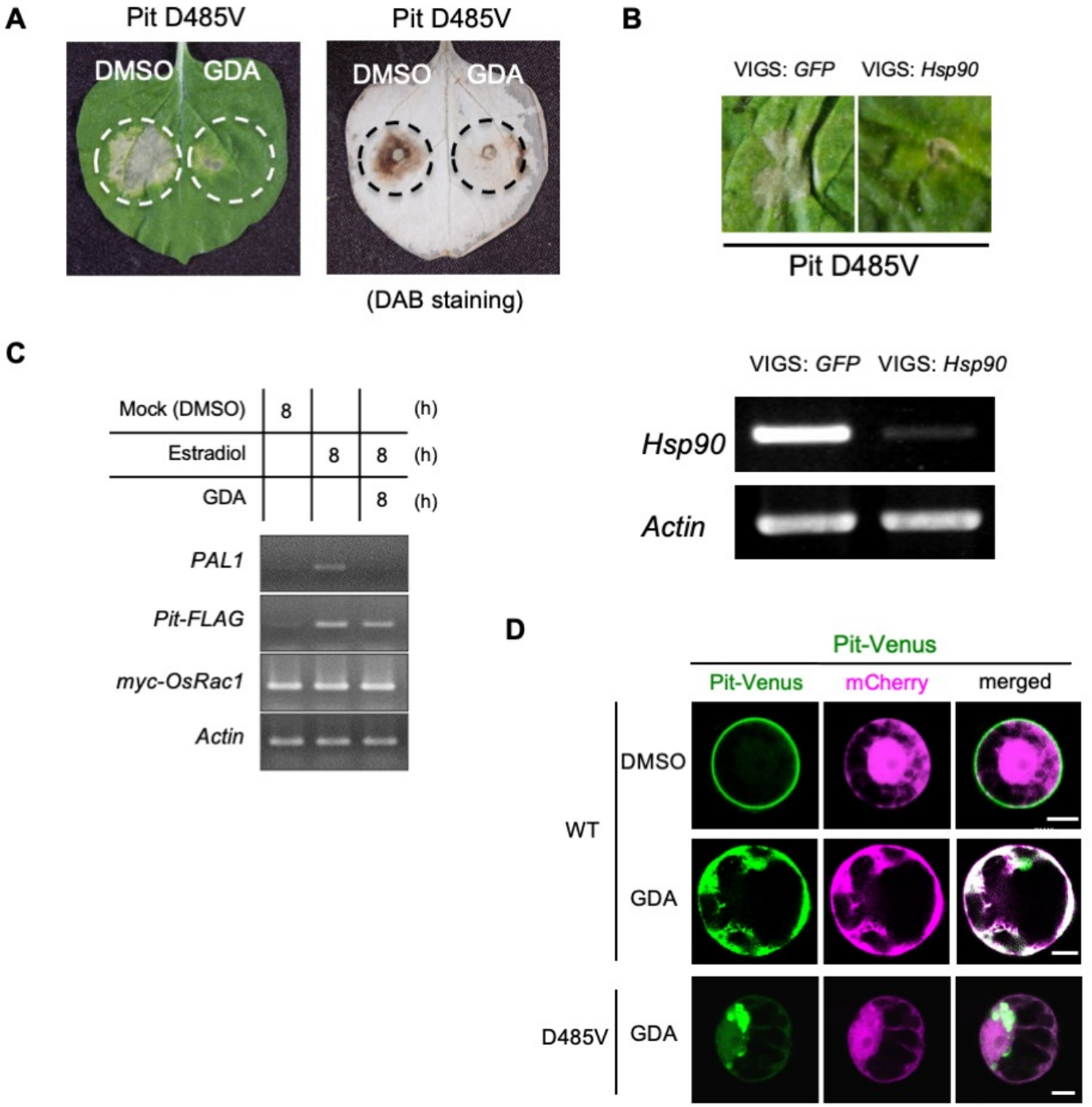

Fig. 5 Hsp90 contributes to Pit-induced immunity

(A) Suppression of Pit-triggered cell death and ROS production by the Hsp90 inhibitor GDA. In the presence or absence of GDA, Pit D485V-induced cell death (left image) and ROS (right image) were examined in *N. benthamiana* leaves. (B) Suppression of Pit D485V-induced cell death by virus-induced gene silencing (VIGS) of Hsp90. *N. benthamiana* plants were inoculated with pGPVX:GFP or pGPVX:Hsp90 (10-186), and three weeks later the upper leaves were infiltrated with a mixture of *Agrobacterium* cultures carrying pGWB2-Pit D485V transgenes. Cell death developed by 7 days after inoculation (upper panels). mRNA expression of *Hsp90* and the internal control *Actin* was detected by RT-PCR (lower panels). (C) Inhibition of *Pit D485V*-induced *PAL1* expression by treatment of with GDA. mRNA expression of *PAL1*, *Pit*, *OsRac1*, *Hsp90*, and *Actin* was detected by RT-PCR. (D) Localization of Pit-Venus in rice protoplasts in the presence of GDA. Pit-Venus was co-transfected with mCherry. Twelve hours after GDA treatment, the transfected cells were observed under a microscope. Scale bars, 5 μm.

Akamatsu et al., Figure S1

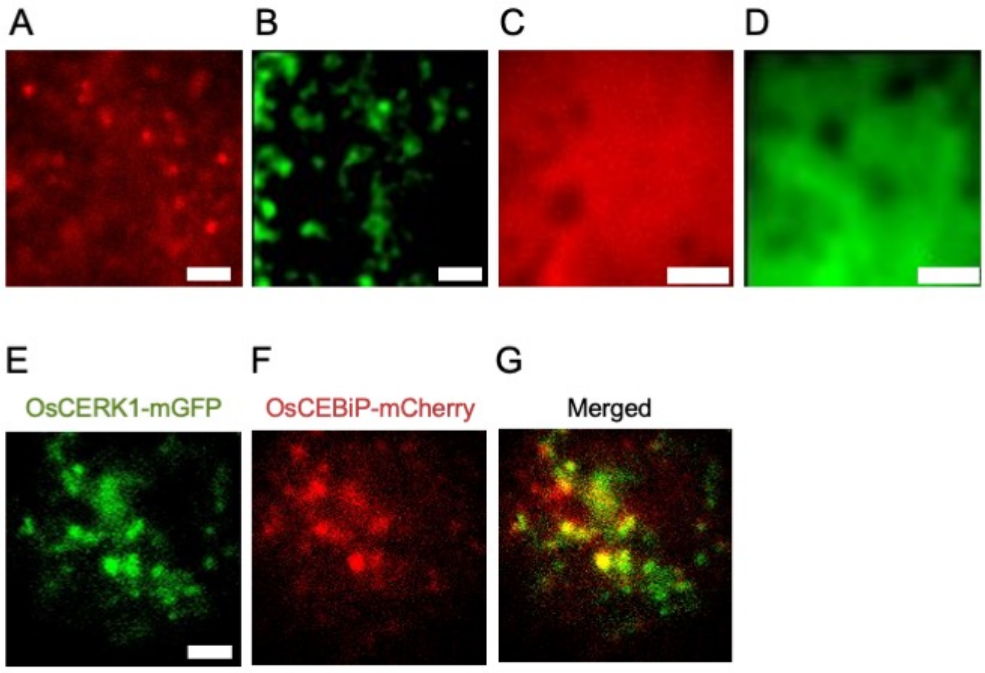

Supplementary Figure 1

VIAFM images of the immune receptors.

Representative image of OsCERK1-mCherry (A), Pit-mEGFP (B), mCherry (C), and mEGFP (D). E-F, co-expression of OsCERK1-mGFP and OsCEBiP-mCherry. Scale bar is 5 μm.